Radiation and Chemical Reaction Effects on Mhd Mixed Convection Flow Past an Inclined Porous Plate Embedded in A Porous Medium with Heat Source and Thermodiffusion

Dr. E. Hemalatha[1], Dr. A. Neeraja[2], Dr. N. Bhaskar Reddy[3]
[1] *Academic Consultant, Sri Venkateswara University, Tirupati – 517502, India*
[2] *Professor, Aditya College of Engineering, Surampalem Kakinada – 533437, India*
[3] *Professor, Sri Venkateswara University, Tirupati – 517502, India*

Abstract – This paper focuses on the radiation and chemical reaction effects on MHD mixed convective flow along inclined porous plate embedded in a porous medium with thermo diffusion in the presence of heat generation. The governing boundary layer equations are reduced to a system of ordinary differential equations using similarity transformations and the resulting equations are then solved numerically using Runge - Kutta fourth order method along with shooting technique. A parametric study is conducted to illustrate the influence of various governing parameters on the velocity, temperature, concentration, skin-friction coefficient, Nusselt number and Sherwood number and discussed in detail.

Key Words – Chemical Reaction, Mixed Convection, Porous Plate, Radiation, Thermo diffusion.

I. INTRODUCTION

In free convection fluid, motion is due to buoyancy effects within the fluid resulting from density variation caused by temperature differences in the fluid, while in forced convection it is externally imposed. The combination of free and forced convection is known as mixed convection. Mixed convection flow has important applications in electronic equipment cooled by a fan and flows in the ocean and in the atmosphere. In mixed convection flows, the forced and free convection effects are of comparable magnitude. Thus, mixed convection occurs if the effect of buoyancy forces on a forced flow or vice versa is significant. The mixed convection on laminar flow takes place in various applications in science and thermal engineering and has drawn attention of researchers in the past decades. Examples of these applications include solar energy systems, atmospheric boundary layer flows, compact heat exchangers, boilers and cooling of electronic devices. Sengupta *et al*. [1] studied the mixed convection boundary layer of linear spatial stability analysis along a heated plate. Ali *et al*. [2] considered the free-forced convective hydro magnetic boundary layer flow towards a stagnation point on a vertical surface in presence of induced magnetic field. Subhashini *et al.* [3] analyzed mixed convection boundary layer flow with buoyancy assisting and opposing effects past a permeable vertical surface. Many researchers investigated the effects of mixed convection viscous boundary layer flow past vertical/ inclined/ horizontal plate and wedge surfaces. Lloyd and Sparrow [4] studied the effects of mixed convective boundary layer flow on vertical surfaces. Schneider [5] analyzed similarity solution for mixed convection boundary layer flow along a horizontal plate. Wilks [6] presented the mixed convection flow along vertical surfaces. Yao [7] studied the mixed convection two-dimensional flow past a flat plate. Ramachandran *et al.* [8] presented the mixed convection in stagnation flows adjacent to vertical surfaces.

From the literature survey it has been observed that the combined heat and mass transfer on mixed convection have been extensively studied on horizontal and vertical configurations and paid little attention on inclined geometries. Laaroussi *et al.* [9] presented numerically the effect of variable density on laminar forced and free convection flow with thin liquid film evaporation in a vertical channel. Ait Hammou *et al.*

[10] studied the numerical solution of evaporation or condensation on laminar mixed convection flow of humid air in a vertical channel. Said *et al.* [11] carried out a numerical study on turbulent free convection boundary layer flow between inclined isothermal plates.

Magnetohydrodynamics has attracted the interest of many researchers because of its wide range of applications in engineering such as astrophysics, purification of crude oil, geothermal reservoirs, ship propulsion, magnetic material processing, cooling of nuclear reactors, MHD generators, Jet printers, petroleum industries, crystal growth, boundary layer control in aerodynamics and so on. Moreover the study of MHD is largely concerned with the flow, heat and mass transfer characteristics in various physical situations. Sri Hari Babu and Ramana Reddy [12] presented the effects of mixed convective mass transfer on hydro magnetic flow past a vertical surface with viscous dissipation in presence of Ohmic heating. Chen *et al*. [13] studied the effects on natural convection heat and mass transfer MHD flow from a permeable, inclined surface with concentration in the presence of variable wall temperature.

Simultaneous heat and mass transfer in porous media with different geometries has attracted many researchers due to its numerous engineering and geophysical applications such as geothermal reservoirs, thermal insulation, packed-bed catalytic reactors, underground energy transport, cooling of nuclear reactors, enhanced oil recovery, drying of porous solids, etc. Lai and Kulacki [14] discussed heat and mass transfer effects on non-Darcy mixed convection boundary layer past vertical plate through a saturated porous medium. Nasir Uddin *et al.* [15] investigated the conjugate heat and mass transfer effects on magneto hydrodynamic mixed convective flow along inclined plate embedded in a porous medium. Sattar and Hossain [16] analyzed the effects of mass transfer with Hall currents on an unsteady free convective boundary layer flow past an accelerated vertical porous plate as time depending temperature and concentration. Vajravelu [17] examined the heat transfer effects on steady flow past a stretching surface through a saturated porous medium. Hong *et al*. [18], Chen and Lin [19] and Jaiswal and Soundalgekar [20] investigated the free convection flows embedded in a porous medium with high porosity.

In many situations there may be an appreciable temperature difference between the surface and ambient fluid. These necessities the consideration of temperature dependent heat sources or sinks which may exert strong influence on the heat transfer characteristics. The study of heat generation or absorption in moving fluids is important in view of several physical problems, such as fluids undergoing exothermic or endothermic chemical reactions. Sparrow and Cess [21] provided similarity solution for stagnation point flow in presence of heat source/sink varying with time. Pop and Soundalgekar [22] presented an unsteady free convection flow past an infinite plate with constant suction in presence of heat source. Reddy *et al.* [23] studied the mass transfer effects on two-dimensional natural convection boundary layer flow along an inclined semi-infinite vertical surface in the presence of heat generation embedded in a porous medium.

Radiation becomes the only significant mode of heat transfer when no medium is present. At high absolute temperature levels such as those prevailing in furnaces, combustion chambers, nuclear explosions and in space applications, the contribution of radiation to heat transfer is very significant. Recent advancement in hypersonic flights, gas cooled nuclear reactors, rocket combustion chambers and missile reentry, have perhaps shifted researchers' attention to thermal radiation as a mode of energy transfer, and emphasize the need for improved understanding of radiative transfer in these processes. Ramachandra Prasad *et al.* [24] studied effects of convective heat and mass transfer on an unsteady MHD radiating flow along a semi-infinite vertical permeable moving plate through a porous medium. Ramana Reddy *et al*. [25] have studied an unsteady free convective MHD viscous incompressible and radiating fluid flow embedded in porous medium with heat generation/absorption. MHD mixed convective heat transfer about a semi-infinite inclined plate in the presence of magnetic field and thermal radiation has been examined by Aydin *et al*. [26]. Recently, Samad and Rahman [27] presented the interaction of the thermal radiation on MHD unsteady boundary layer flow along vertical porous plate immersed in a porous medium. Uddin and Kumar [28] studied the effects of free convection MHD radiating flow of an isothermal cylinder embedded in a porous medium.

It is essential to study the heat and mass transfer problems with chemical reaction because of its growing need in chemical and hydrometallurgical industries. The study of such process takes place in number of chemical technologies such as food processing, polymer production, the manufacturing of ceramics or glassware and so on. Singh *et al.* [29] presented absorption of chemical reaction and radiation effects on magnetohydrodynamic natural convective heat and mass transfer flow along a semi-infinite vertical moving plate in the presence of suction depending on time. Ibrahim *et al*. [30] presented an unsteady magneto hydrodynamic natural convection chemical reacting and radiation absorbing fluid flow along a continuously moving permeable surface with heat source and time dependent suction. Rajeswari *et al*. [31] investigated the effect of chemical reaction on unsteady MHD natural convection boundary layer of radiation absorption fluid flow along a semi-infinite vertical permeable moving plate in the presence of heat source with suction. Recently, Kandasamy et al. [32, 33] presented chemical reaction effects on heat and mass transfer boundary layer flows with heat source. Gangadhar and Bhaskar reddy [34] analyzed the chemically reaction, heat and mass transfer effects on MHD flows along a moving vertical plate embedded in a porous medium with suction. Patil and Kulkarni [35] investigated the effects of chemically reacting natural convective polar fluid flow in a porous medium with internal heat generation.

Thermophoresis is a phenomenon which causes small particles to be driven away from a hot surface and towards a cold one. Small particles, such as dust, when suspended in a gas with a temperature gradient, experience a force in the direction opposite to the temperature gradient. This phenomenon has many practical applications in removing small particles from gas streams, in determining exhaust gas particle trajectories from combustion devices, and in studying the particulate material deposition on turbine blades. Recently, Chamkha *et al*. [36] studied the effect of thermophoretic particle deposition in free convection boundary layer from a vertical flat plate embedded in a porous medium. Bakier *et al*. [37] dealt with the effects of thermophoresis particle deposistion on MHD boundary layer flow past a vertical flat plate through a fluid-saturated porous medium. Lin *et al* [38] investigated the suppression of particle deposition from flow through a tube with circular cross-section when the wall temperature exceeds that of the gas. Seddek [39] presented the effects of thermophoresis of chemically reacting MHD flow over a heat surface in the presence of variable viscosity and heat source/absorption. Alam *et al*. [40] considered the effects heat thermophoresis on magneto hydrodynamic boundary flow with heat and mass transfer past a semi-infinite permeable inclined flat surface. Loganathan and Arasu [41] presented the effect of thermophoresis on non-Darcy free-forced convective heat and mass transfer along a porous wedge with suction or injection.

II. MATHEMATICAL ANALYSIS

A steady two-dimensional MHD laminar mixed convective flow of a viscous incompressible, electrically conducting, radiating and chemically reacting fluid past a semi-infinite inclined porous plate embedded in porous mdium with an acute angle α to the vertical is considered. The flow is assumed to be in the x - direction, which is taken along the semi-infinite inclined porous plate and y - axis normal to it. The velocity components in the directions of flow and normal to the flow are u and v respectively. A uniform magnetic field strength B_0 is applied normal to the direction of y-axis.

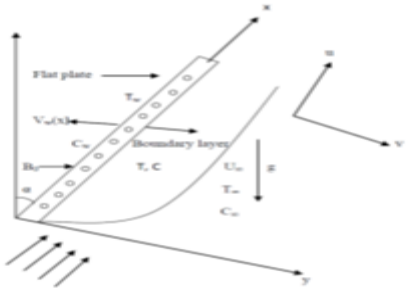

Fig. 1 Schematic diagram of the physical model

The fluid is assumed to be slightly conducting, so that the magnetic Reynolds number is much less than unity, and hence the induced magnetic field is negligible in comparison with applied magnetic field. The external flow with a uniform velocity U_∞ takes place in the direction parallel to the inclined plate. It is assumed that T and C are the temperature and concentration of the fluid which are the same, everywhere in the fluid. The surface is maintained at a constant temperature T_w, which is higher than the constant temperature T_∞ and the concentration C_w is

greater than the constant concentration C_∞ of the surrounding fluid. It is assumed that there is no applied voltage which implies the absence of electrical field. The fluid is considered to be a gray, absorbing emitting radiation but non-scattering medium and the Rosseland approximation is used to describe the heat flux in the energy equation.

Under the above assumptions and usual Boussinesq's approximation, the governing boundary layer equations describing the flow can be written as

Continuity equation

$$\frac{\partial u}{\partial x}+\frac{\partial v}{\partial y}=0 \tag{2.1}$$

Momentum equation

$$u\frac{\partial u}{\partial x}+v\frac{\partial u}{\partial y}=\upsilon\frac{\partial^2 u}{\partial y^2}+g\beta\left(T-T_\infty\right)\cos\alpha+g\beta^*\left(C-C_\infty\right)\cos\alpha-\left(\frac{\sigma B_0^2}{\rho}+\frac{\upsilon}{K^*}\right)u \tag{2.2}$$

Energy equation

$$u\frac{\partial T}{\partial x}+v\frac{\partial T}{\partial y}=\frac{k}{\rho C_p}\frac{\partial^2 T}{\partial y^2}+\frac{Q_0}{\rho C_p}\left(T-T_\infty\right)-\frac{1}{\rho C_p}\frac{\partial q_r}{\partial y} \tag{2.3}$$

Species equation

$$u\frac{\partial C}{\partial x}+v\frac{\partial C}{\partial y}=D\frac{\partial^2 C}{\partial y^2}-\frac{\partial}{\partial y}\left\{V_T\left(C-C_\infty\right)\right\}-Kr'C \tag{2.4}$$

where υ is the kinematics viscosity, g is the acceleration due to gravity, β, β^* are the volumetric coefficients of thermal and concentration expansions, respectively, T, C are the temperature and concentration of the fluid, respectively, T_∞, C_∞ are the free stream temperature and concentrations respectively, σ is the electrical conductivity, B_0 - the magnetic induction, ρ is the fluid density of the fluid, K^* is permeability of the porous medium, k is the thermal conductivity of the fluid, C_p is the specific heat at constant pressure, Q_0 is the heat generation constant, q_r is the radiative heat flux, D is the mass diffusivity, V_T is the thermophoretic velocity and Kr' is the chemical reaction rate of the species concentration.

The third and fourth terms on the RHS of the momentum equation (2.2) denote the thermal and concentration buoyancy effects, and last two terms of the momentum equation represent magnetic field and porous effects, respectively. Also the last two terms of on the RHS of the energy equation (2.3) represent the heat absorption and thermal radiation effects, respectively. The last two terms on the RHS of the species equation (2.4) represents the thermophoretic and chemical reaction effects, respectively. It is assumed that the physical properties, that is, viscosity, heat capacity, thermal diffusivity and the mass diffusivity of the fluid remain invariant throughout the fluid.

The boundary conditions for the velocity, temperature and concentration fields are

$u=0$, $v=\pm v_w(x)$, $T=T_w$, $C=C_w$ *at* $y=0$

$u=U_\infty$, $T=T_\infty$, $C=C_\infty$, *as* $y\to\infty$ (2.5)

In addition, U_∞ is the free stream velocity and $v_w(x)$ represent the permeability of the porous plate where its sign indicates suction (< 0) or blowing (> 0), subscripts w and ∞ refer to the wall and boundary layer edge, respectively.

The effects of thermophoresis are being taken into account to help in the understanding of the mass deposition variation on the surface. The effect of thermophoresis is usually prescribed by means of an average velocity that a particle will acquire when exposed to a temperature gradient. For boundary layer analysis it is found that the temperature gradient along the plate is much lower than the temperature gradient normal to the surface, *i.e.*, $\frac{\partial T}{\partial y}>>\frac{\partial T}{\partial x}$. So the component of thermophoretic velocity along the plate is negligible compared to the component of its normal to the surface. As a result, the thermophoretic velocity V_T which appears in the equation (2.4) can be written as

$$V_T=-k\upsilon\frac{\Delta T}{T_{ref}}=-\frac{k\upsilon}{T_{ref}}\frac{\partial T}{\partial y} \tag{2.6}$$

where T_{ref} is some reference temperature and k is the thermophoretic coefficient which is defined by[42].

By using the Rosseland approximation (Brewster [43]), the heat flux q_r is given by

$$q_r=\frac{4\sigma^*}{3k^*}\frac{\partial T^4}{\partial y} \tag{2.7}$$

Where σ^* is the Stephen-Boltzmann constant and k^* is the mean absorption. It should be noted that by using the Rosseland approximation, the present analysis is limited to optically thick fluids. If the temperature differences within the flow are sufficiently small, then equation (2.3) can be linearized by expanding T^4 into the Taylor series about T_∞, which after neglecting higher order terms takes the form

$$T^4 = 4T_\infty^3 T - 3T_\infty^4 \tag{2.8}$$

In view of the equations (2.7) and (2.8), the equation (2.3) reduces to

$$u\frac{\partial T}{\partial x} + v\frac{\partial T}{\partial y} = \alpha\frac{\partial^2 T}{\partial y^2} + \frac{Q_0}{\rho C_p}(T - T_\infty) + \frac{16\sigma^* T_\infty^3}{3k^*\rho c_p}\frac{\partial^2 T}{\partial y^2} \tag{2.9}$$

The continuity equation (2.1) is satisfied by the Cauchy Riemann equations

$$u = \frac{\partial \psi}{\partial y} \text{ and } v = -\frac{\partial \psi}{\partial x} \tag{2.10}$$

where $\psi(x,y)$ is the stream function.

In order to write the governing equations and the boundary conditions in dimensionless form, the following dimensionless quantities are introduced.

$$\eta = y\sqrt{\frac{U_\infty}{\upsilon x}}, \qquad \psi = \sqrt{\upsilon x U_\infty}\, f(\eta),$$

$$u = U_\infty f'(\eta), \quad v = \frac{1}{2}\sqrt{\frac{\upsilon U_\infty}{x}}\left(\eta f' - f\right),$$

$$\theta(\eta) = \frac{T - T_\infty}{T_w - T_\infty}, \qquad \phi(\eta) = \frac{C - C_\infty}{C_w - C_\infty},$$

$$M_x = \frac{\sigma B_0^2 x}{\rho U_0},\ Gr_x = \frac{g\beta(T_w - T_\infty)x}{U_\infty^2}, \tag{2.11}$$

$$Gc_x = \frac{g\beta^*(C_w - C_\infty)x}{U_\infty^2}, \qquad K_x = \frac{\upsilon x}{K^* U_\infty},$$

$$\Pr = \frac{\upsilon\rho C_p}{k}, \quad Sc = \frac{\upsilon}{D},$$

$$Q_x = \frac{Q_0 x}{U_\infty \rho C_p},\ Kr_x = \frac{Kr' x}{U_\infty},\ R = \frac{4\sigma^* T_\infty^3}{3k^* k},$$

$$\tau = \frac{k\left(T_w - T_\infty\right)}{T_{ref}},$$

where prime denotes differentiation with respect to η, η - the similarity variable, $f(\eta)$ - the dimensionless stream function, $f'(\eta)$ - the dimensionless velocity, $\theta(\eta)$- the dimensionless temperature, $\varphi(\eta)$ - the dimensionless concentration M_x - the local magnetic field parameter, Gr_x - the local thermal Grashof number, Gc_x - the modified Grashof number, K_x – the permeability parameter, Pr - the Prandtl number, Sc - the Schmidt number, Q_x - the heat generation parameter, Kr_x - the chemical reaction parameter, R - the radiation parameter and τ - thermophoretic parameter.

In the view of the above similarity transformations, the equations (2.2), (2.9) and (2.4) reduce to

$$f''' + \frac{1}{2}ff'' + Gr_x\theta\cos\alpha + Gc_x\varphi\cos\alpha - \left(M_x + K_x\right)f' = 0 \tag{2.12}$$

$$\left(4R+1\right)\theta'' + \frac{1}{2}\Pr\, f\theta' + \Pr Q_x\theta = 0 \tag{2.13}$$

$$\varphi'' + Sc\left(\frac{1}{2}f - \tau\theta'\right)\varphi' - Sc\varphi\left(\tau\theta'' - Kr_x\right) = 0 \tag{2.14}$$

The corresponding boundary conditions are

$f = f_w$, $f' = 0$, $\theta = 1$, $\varphi = 1$ at $\eta = 0$ (2.15)

$f' \to 1$, $\theta \to 0$, $\varphi \to 0$ as $\eta \to \infty$ (2.16)

$f_w = -v_w(x)\sqrt{x/\upsilon U_\infty}$ is the non dimensional wall mass transfer coefficient such that $f_w > 0$ indicates wall suction and $f_w < 0$ indicates wall injection or blowing.

For the type of boundary layer flow under consideration the skin-friction coefficient, Nusselt number and Sherwood number are important parameters. They are described as follows.

By employing definition of wall shear stress $\tau_w = \mu(\partial u/\partial y)_{y=0}$ along with Fourier's law $q_w = -k(\partial T/\partial y)_{y=0}$ and Fick's law $J_s = -D(\partial c/\partial y)_{y=0}$ the non-dimensional forms of local skin-friction coefficient is $C_f = 2\,\mathrm{Re}^{-1/2} f''(0)$, local Nusselt number is $N_u = -2\,\mathrm{Re}^{1/2}\theta'(0)$ and local Sherwood number is $S_h = -2\,\mathrm{Re}^{1/2}\phi'(0)$, where $\mathrm{Re}_x = xU_\infty/\upsilon$ is the local Reynolds number.

It can be noted that the local parameters Ha_x, Gr_x, Gc_x, K_x, Q_x and Kr_x in the equations (2.12) - (2.14) are functions of x and generate local similarity solution. In order to have a true similarity solution all the parameters Ha_x, Gr_x, Gc_x, K_x, Q_x and Kr_x must be constant and we therefore assume

$$\sigma = \frac{b}{x}, \quad \beta = \frac{c}{x}, \ \beta^* = \frac{d}{x},$$

$$K^* = \frac{a}{x}, \ Q_0 = \frac{e}{x}, \quad Kr' = \frac{m}{x}$$

where *a, b, c, d, e* and *m* are the constants with appropriate dimensions.

III. SOLUTION OF THE PROBLEM

The non-linear boundary value problem given by equations (2.12) - (2.14) and boundary conditions (2.15) does not possess a closed form analytical solution. Therefore it has been solved numerically by using fourth order Runge-Kutta scheme together with Newton Raphson shooting method. First of all, writing higher order non-linear differential equations (2.12), (2.13) and (2.14) into simultaneous first order differential equations as follows.

Let $f = y_1$, $f' = y_2$, $f'' = y_3$, $\theta = y_4$, $\theta' = y_5$, $\varphi = y_6$, $\varphi' = y_7$.

Thus, the corresponding first order differential equations are

$$\frac{dy_1}{d\eta} = y_2,$$

$$\frac{dy_2}{d\eta} = y_3,$$

$$\frac{dy_3}{d\eta} = -\{\frac{1}{2} y_1 y_3 + Gr_x y_4 \cos\alpha + Gc_x y_6 Cos\alpha - (M_x + K_x) y_2\},$$

$$\frac{dy_4}{d\eta} = y_5,$$

$$\frac{dy_5}{d\eta} = \frac{-1}{(4R+1)}\{\frac{1}{2}\Pr y_1 y_5 + \Pr Q y_4\},$$

$$\frac{dy_6}{d\eta} = y_7,$$

$$\frac{dy_7}{d\eta} = -\{Sc(\frac{1}{2} y_1 - \tau y_5) y_7 - Scy_6(\tau \frac{dy_5}{d\eta} + Kr_x\},$$

subject to following initial conditions

$$y_1(0) = f_w, \ \ y_2(0) = 0, \quad y_4(0) = 1, \ y_6(0) = 1,$$

$$y_2(\infty) = 1, \ y_4(\infty) = 0, \ \ y_6(\infty) = 0$$

Then the set of above equations are transformed into initial value problem by applying the shooting technique (Jain *et al*. [44]). We have chosen a step size of $\Delta\eta$ = 0.01 to satisfy the convergence criterion of 10^{-6} in all cases. From the process of numerical computation, the skin-friction coefficient, Nusselt number and Sherwood number which are respectively proportional to $f''(0)$, $-\theta'(0)$, and $-\varphi'(0)$ are also sorted out and their numerical values are presented in a tabular form.

IV. RESULTS AND DISCUSSION

In order to get a physical insight into the problem, a parametric study is conducted to illustrate the effects of different governing parameters viz local magnetic field parameter *M*, the thermal Grashof number Gr_x, the modified Grashof number Gc_x, internal heat generation parameter *Q*, permeability of the porous medium *K*, the Prandtl number *Pr*, the Schmidt number *Sc*, the chemical reaction parameter *Kr*, the thermophoretic parameter τ and the non-dimensional wall mass transfer coefficient f_w and radiation parameter *R* upon the nature of flow and transport, the numerical results are depicted graphically in Figs. 2-26. Throughout the calculations, the parametric values are chosen as for *Gr* =*Gc*=0.87, *M*= 0. 1, *K*=0.01, α=30^0, *Pr*= 0.71, *Q* =0.5, *R*=1.0, f_w = 0.5, *Kr*=0.1, *Sc* = 0.6 τ = 0.1. All the graphs therefore correspond to these values unless specifically indicated on the appropriate graph. In order to ascertain the accuracy of the numerical results, the present study is compared with the previous study. The velocity profiles for *Gr* = 2.0, *Gc* = 2.0, *K*=0.5, *M*= 0.01, *Q* =0.5, α=30^0, *Pr*= 0.71, f_w = 0.5, *Sc* = 0.22. τ = 0.1, *R*=0, *K*r=0 are compared with the available solution of Nasir Uddin *et al.* [45] in Fig. 2. It is observed that the present results are in good agreement with that of Nasir Uddin *et al.* Numerical results for the skin-friction coefficient, the Nusselt number, the Sherwood number and the plate surface temperature for various values of physical parameters are reported in Tables.

The effect of magnetic parameter (*M*) on the velocity field is shown in Fig. 3. It illustrates that the velocity decreases with an increase in the magnetic parameter, because the magnetic parameter is found to retard the velocity at all points of the flow field. It is because that the application of transverse magnetic field will result in a resistive type force (Lorentz force) similar to drag force which tends to resist the fluid flow and thus reducing its velocity. Also, the boundary layer thickness decreases with an increase in the

magnetic parameter. Fig. 4 represents the effect of the magnetic parameter on the temperature. It is noticed that the temperature of the fluid increases as the magnetic parameter increases. This is due to the fact that the applied magnetic field tends to heat the fluid, and thus reduces the heat transfer from the wall.

Fig. 5 and Fig. 6 illustrate the effect of the thermal Grashof number (*Gr*) and mass (solutal) Grashof number (*Gc*) on the velocity field. The thermal Grashof number signifies the relative effect of the thermal buoyancy force to the viscous hydrodynamic force and the mass (solutal) Grashof number defines the ratio of species buoyancy force to the viscous hydrodynamic force in the boundary layer. It is observed that with an increase in *Gr* or *Gc*, there is an increase in the velocity. It is due to the fact that an increase in the values of *Gr* or *Gc* has the tendency to increase the thermal and mass buoyancy effects. Further, the velocity increases rapidly and suddenly falls near the boundary and then approaches the far field boundary condition due to favorable buoyancy force with an increase in *Gc*. Fig. 7 and Fig. 8 represents the temperature for different values of the Grashof number and modified Grashof number respectively. It is observed that the thermal boundary layer decreases with an increasing thermal Grashof number or modified Grashof number. The effect of buoyancy parameters (*Gr*, *Gc*) on the concentration field is illustrated in Fig. 9 and Fig. 10. It is noticed that concentration boundary layer thickness decreases with an increase in the thermal or solutal Grashof numbers. It is due to the fact that an increase in the values of Grashof number or modified Grashof number has the tendency to increase the mass buoyancy effect.

Fig. 11 illustrates the effect of permeability parameter (*K*) on the velocity. It is noticed that as the permeability parameter increases, the velocity decreases. The parameter *K* as defined in (2.11) is inversely proportional to the actual permeability K^* of the porous medium. An increase in *K* will therefore decrease the resistance of the porous medium (as the permeability physically becomes less with increasing K^*) which will tend to decelerate the flow and reduce the velocity. Fig. 12, display the effect of temperature across the boundary layer for different values of the permeability parameter. It is noticed that an increase in the permeability parameter leads to an increase in the fluid temperature.

Fig. 14 shows the effect of the Prandtl number (*Pr*) on the temperature. It is observed that, an increase in the Prandtl number results in decrease of the thermal boundary layer, and hence temperature decreases. Prandtl number signifies the ratio of momentum diffusivity to thermal diffusivity. In heat transfer problems, the Prandtl number controls the relative thickening of the momentum and thermal boundary layers. The reason is that, smaller values of *Pr* are equivalent to increase the thermal conductivities, when Prandtl number is small, heat is able to diffuse away from the heated surface more rapidly than for higher values of *Pr*. As *Pr* enhances, it can be seen from Fig. 13 that the velocity reduces. This is due to the fact that with an increase in *Pr*, rate of viscous diffusion exceeds the rate of thermal diffusion and hence it is seen that velocity decreases throughout the regime.

The positive value of (*Q*) represents heat source *i.e*. heat generation in the fluid. From Fig. 15, it is observed that due to increase in heat generation parameter enhances the thermal buoyancy force of driving force due to mass density variations which are coupled to the temperature distribution which in turn gives rises the velocity in the boundary layer. The effect of the heat generation parameter on the temperature is shown in Fig. 16. It is seen that with an increase in the heat generation parameter, the temperature increases. This is due to the fact that the presence of a heat source on the flow field, the thermal state of the fluid increases causing the thermal boundary layer to increase. The influence of heat generation parameter on concentration is shown in Fig. 17. It is seen that the concentration decreases as *Q* increase.

The influence of thermal radiation parameter *R* on the velocity and temperature is shown in Fig. 18 and Fig. 19. The radiation parameter defines the relative contribution of conduction heat transfer to thermal radiation transfer. It is obvious that, with an increase in the radiation parameter results an increase in both the velocity and temperature within the boundary layer.

The effect of chemical reaction parameter (*Kr*) on the concentration is presented in Fig. 20. It is observed that the species concentration decreases with an increase in the chemical reaction parameter. Physically this shows that an increase in chemical reaction parameter breaks up the bonds between the

atoms and thus the density of the species dilutes and thereby decreases the concentration of the fluid.

The effect of the Schmidt number (*Sc*) on the velocity, temperature and concentration are shown in Figs. 21-23, respectively. Moreover, the Schmidt number is an important parameter in heat and mass transfer processes as the Schmidt number embodies the ratio of momentum to mass diffusivity. The Schmidt number quantifies the relative effectiveness of momentum and mass transport by diffusion in the hydrodynamic (velocity) and concentration (species) boundary layers. Its effect on the species concentration has similarities to the Prandtl number effect on the temperature. As the Schmidt number increases the concentration decreases. This causes the concentration buoyancy effects to decreases yielding reduction in the fluid velocity resulting in less induced flow and higher fluid temperatures.

The influence of thermophoretic parameter (τ) on the concentration is shown in Fig. 24. It is seen that the concentration decreases with an increase of the thermophoretic parameter due to the small temperature difference between the hot fluid and the free stream.

Figs. 25-27 illustrate the effect of suction parameter (f_w>0) on the velocity, temperature and concentration. It is observed that with an increase in the suction parameter velocity, temperature and concentration decreases. This is due to the fact that with an increase in suction rate, more warm fluid is pushed towards the wall where the buoyancy forces acts to reduce the fluid velocity due to influence of high viscosity. This effect also reduces the wall sear stress. An increase in the suction parameter destroys the momentum transfer and stabilizes the boundary layer flow on the surface.

From Table 1, it is observed that the local skin-friction, Nusselt number and Sherwood number coefficient increase with an increase in the buoyancy forces (*Gc* or *Gr*). As the magnetic parameter (*M*) increases, the skin-friction, Nusselt number and Sherwood number decrease. It can be seen that the local skin-friction coefficient, Nusselt number and Sherwood number decrease with an increase in the porous medium parameter (*K*).It is noted that an increase in suction parameter (f_w>0) increase the skin friction coefficient, Nusselt number Sherwood number.

From Table 2, it is found that the local skin-friction coefficient, Nusselt number and Sherwood number decrease with an increase in the Prandtl number (*Pr*). It is noticed that the skin-friction and Sherwood number increase, where as Nusselt number decreases with an increase in the internal heat generation parameter (*Q*). It is observed that the skin-friction coefficient and Sherwood number increase, whereas Nusselt number decreases with an increase in the radiation parameter(*R*).

From Table 3, it is clear that both the skin friction coefficient and Nusselt number decrease while Sherwood number increases as the Schmidt number (*Sc*) or chemical reaction parameter (*Kr*) or thermophoretic parameter (τ) increases.

V. CONCLUSION

The present model helps us to understand numerically as well as physically the effect of the radiation and chemical reaction on a steady magneto hydrodynamic heat and mass transfer flow of laminar mixed convective boundary layer flow of viscous incompressible, electrically conducting fluid past an inclined porous plate with thermo diffusion. The set of governing equations and the boundary condition are reduced to ordinary differential equations with appropriate boundary conditions using similarity transformations. The resultant dimensionless equations are then solved numerically by shooting technique with Runge-Kutta scheme. A comparison with previously published work is performed and the results are found to be in good agreement. Based on the obtained results, the following conclusions may be drawn.

- The velocity, skin friction coefficient, rate of heat transfer as well as the rate of mass transfer decreases whereas the temperature increases with an increase in the magnetic parameter.
- As mass (solutal) Grashof number increases the velocity increases near the plate and then it decreases smoothly away from the plate, while velocity increases throughout the boundary layer with an increase in the thermal Grashof number.
- An increase in the mass (solutal) Grashof number or thermal Grashof number causes a fall in the temperature and concentration, whereas a rise in

the skin friction coefficient, rate of heat transfer, as well as rate of mass transfer.

- An increase in the permeability parameter reduces the velocity, skin friction coefficient, heat transfer coefficient and the mass transfer coefficient but enhances the temperature.
- An increase in the Prandtl number decreases all the physical quantities.
- The velocity, temperature as well as the skin friction coefficient and the mass transfer rate increases whereas the concentration and local heat transfer rate decreases with an increase in the heat generation or radiation parameter.
- With an increase in the heat generation parameter the concentration decreases.
- The velocity as well as concentration decreases while the temperature increase with an increase in the Schmidt number.
- There is a decrease in the concentration with an increase in the chemical reaction parameter or thermophoretic parameter
- With an increase in the local chemical reaction parameter or Schmidt number or thermophoretic parameter there is a decrease in the skin friction coefficient, Nusselt number and an increase in the Sherwood number.
- As the suction parameter increases, skin friction coefficient, Nusselt number and Sherwood number increase while the velocity, temperature and concentration decrease.

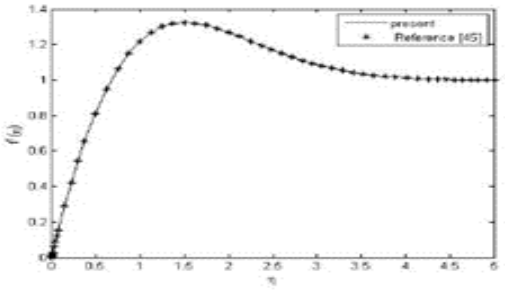

Fig. 2 Comparison of velocity distribution

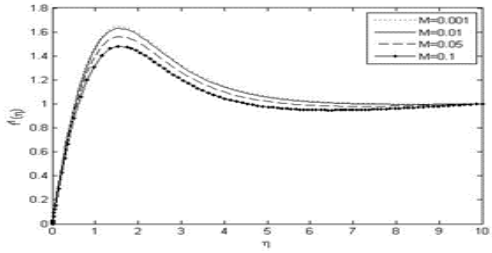

Fig. 3 Velocity profiles for different values of *M*

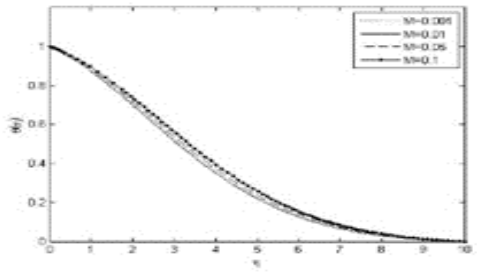

Fig. 4 Temperature profiles for different values of *M*

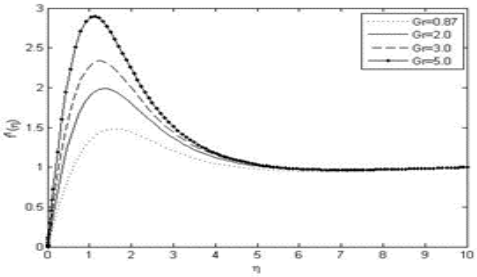

Fig. 5 Velocity profiles for different values of *Gr*

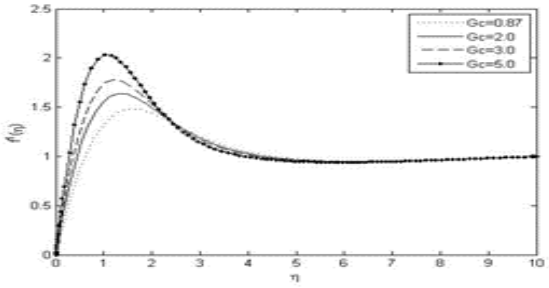

Fig. 6 Velocity profiles for different values of *Gc*

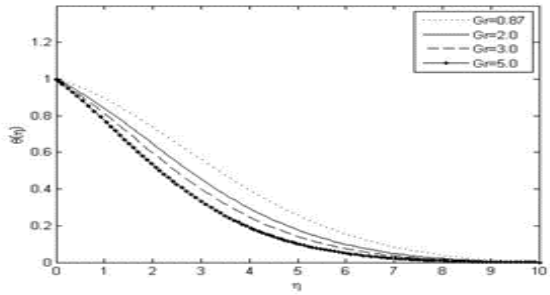

Fig.7 Temperature profiles for different values of *Gr*

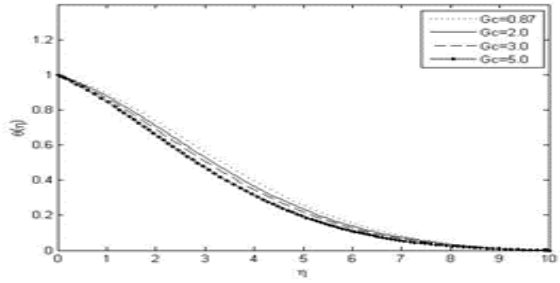

Fig. 8 Temperature profiles for different values *Gc*

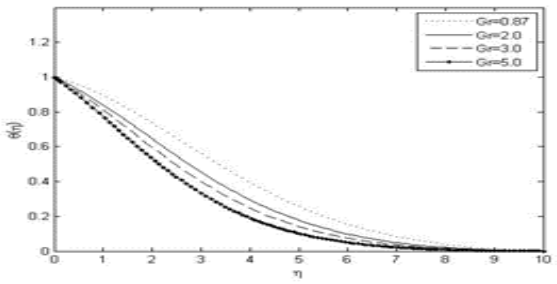

Fig. 9 Concentration profiles for different values of *Gr*

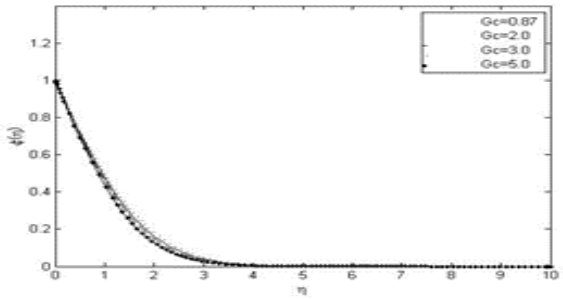

Fig. 10 Concentration profiles for different values of *Gc*

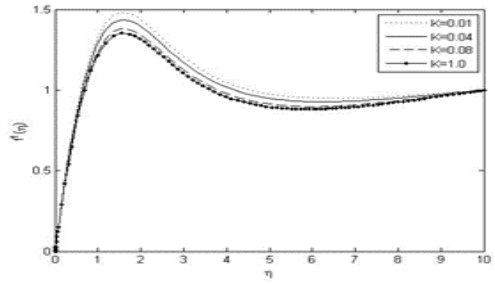

Fig. 11 Velocity profiles for different values of *K*

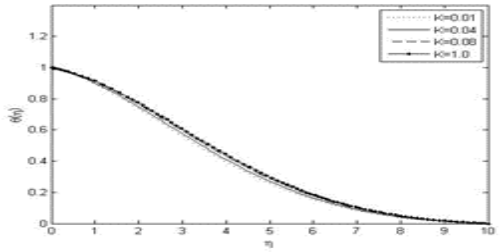

Fig. 12 Temperature profiles for different values of *K*

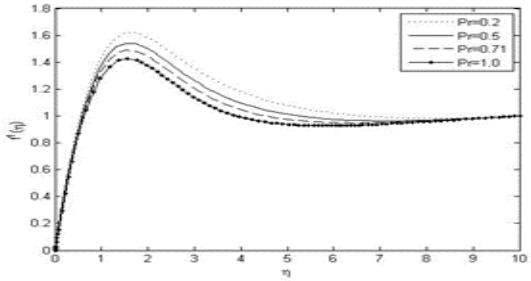

Fig. 13 Velocity profiles for different values of *Pr*

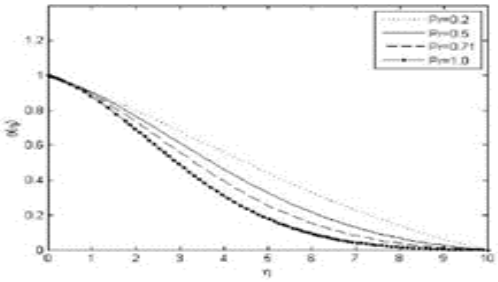

Fig.14 Temperature profiles for different values of *Pr*

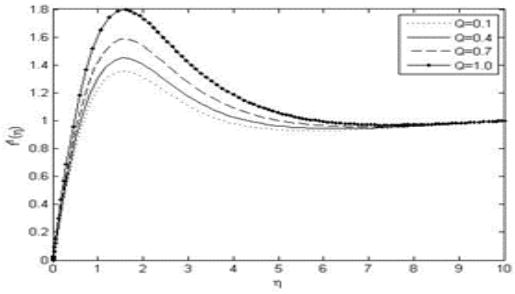

Fig. 15 Velocity profiles for different values of *Q*

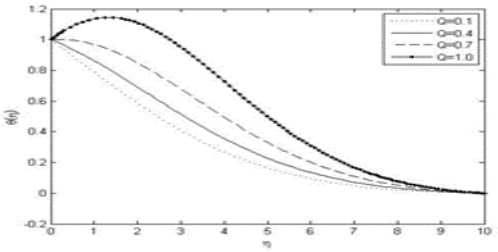

Fig. 16 Temperature profiles for different values of *Q*

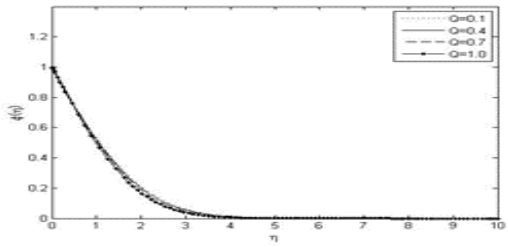

Fig. 17 Concentration profiles for different values of *Q*

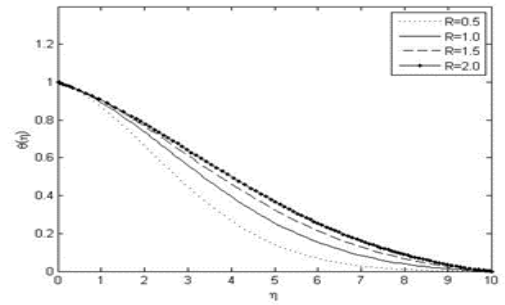

Fig. 18 Velocity profiles for different values of *R*

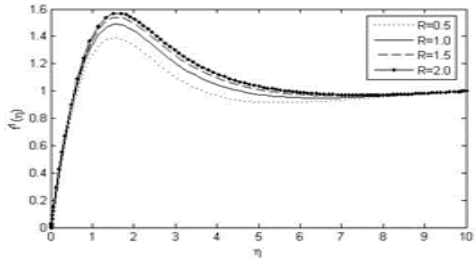

Fig. 19 Temperature profiles for different values of *R*

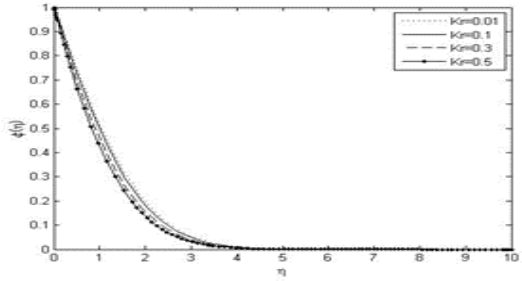

Fig. 20 Concentration profiles for different values of *Kr*

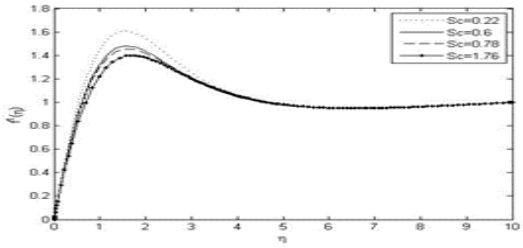

Fig. 21 Velocity profiles for different values of *Sc*

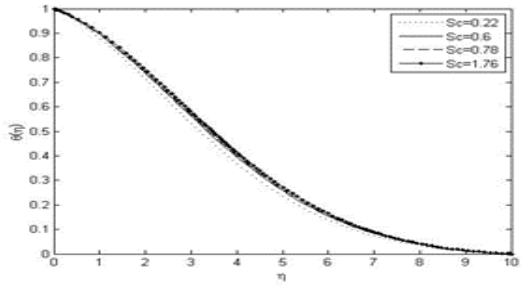

Fig. 22 Temperature profiles for different values of *Sc*

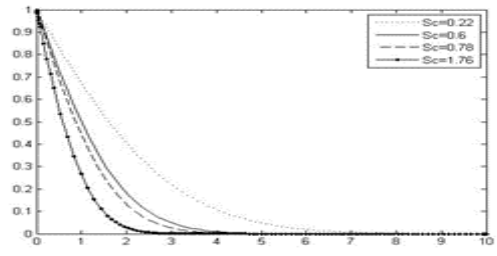

Fig. 23 Concentration profiles for different values of *Sc*

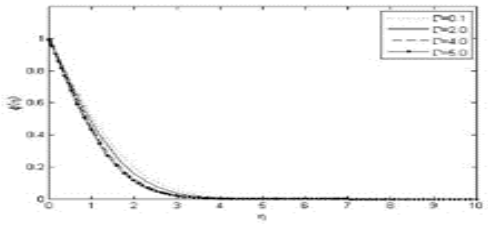

Fig. 24 Concentration profiles for different values of τ

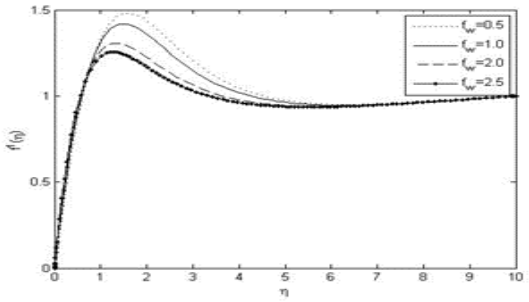

Fig. 25 Velocity profiles for different values of f_w

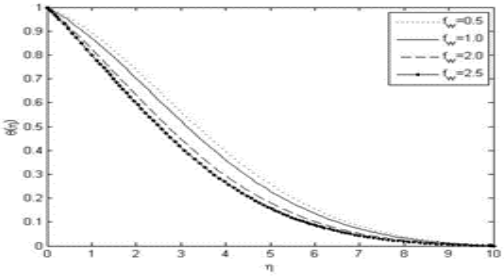

Fig. 26 Temperature profiles for different values of f_w

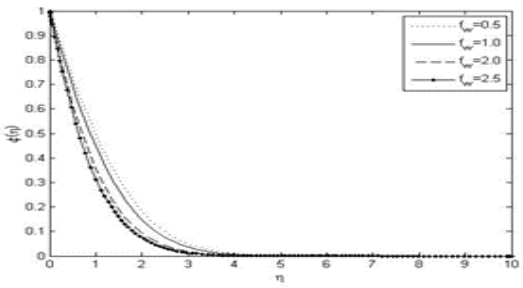

Fig. 27 Concentrations profiles for different values of f_w

Table 1: Numerical values of $f''(0)$, $-\theta'(0)$ and $-\varphi'(0)$ for Pr= 0.71, α=30^0, Q =0.5, R=1.0, f_w = 0.5, Kr=0.1, Sc = 0.6 τ = 0.1

Gc	*Gr*	*M*	*K*	f_w	$f''(0)$	$-\theta'(0)$	$-\varphi'(0)$
0.87	0.87	0.1	0.01	0.5	2.221793	0.074524	0.578133
2.0	0.87	0.1	0.01	0.5	2.899177	0.091296	0.605090
3.0	0.87	0.1	0.01	0.5	3.460697	0.103610	0.625349
5.0	0.87	0.1	0.01	0.5	4.508549	0.123744	0.659311
0.87	0.87	0.1	0.01	0.5	2.221793	0.074524	0.578133
0.87	2.0	0.1	0.01	0.5	3.356764	0.128842	0.639806
0.87	3.0	0.1	0.01	0.5	4.234310	0.159216	0.678375
0.87	5.0	0.1	0.01	0.5	5.801055	0.200977	0.735831
0.87	0.87	0.001	0.01	0.5	2.427690	0.097084	0.595850
0.87	0.87	0.01	0.01	0.5	2.407343	0.095025	0.594164

0.87	0.87	0.05	0.01	0.5	2.320923	0.085889	0.586849
0.87	0.87	0.1	0.01	0.5	2.221793	0.074524	0.578133
0.87	0.87	0.1	0.04	0.5	2.166794	0.067758	0.573137
0.87	0.87	0.1	0.08	0.5	2.098349	0.058820	0.566752
0.87	0.87	0.1	0.01	0.5	2.221793	0.074524	0.578133
0.87	0.87	0.1	0.01	1.0	2.402005	0.099446	0.678866
0.87	0.87	0.1	0.01	2.0	2.742168	0.153422	0.900122
0.87	0.87	0.1	0.01	2.5	2.903299	0.182384	1.019239

Table 2: Numerical values of $f''(0)$, $-\theta'(0)$ and $-\varphi'(0)$ for for $Gr = Gc = 0.87$, $M = 0.1$, $K = 0.01$, $\alpha = 30^0$, $f_w = 0.5$, $Kr = 0.1$, $Sc = 0.6$ $\tau = 0.1$.

Pr	*Q*	*R*	$f''(0)$	$-\theta'(0)$	$-\varphi'(0)$
0.2	0.5	1.0	2.347548	0.084355	0.546870
0.5	0.5	1.0	2.283498	0.075632	0.538743
0.71	0.5	1.0	2.236659	0.075288	0.533045
1.0	0.5	1.0	2.179124	0.077419	0.526031
0.71	0.1	1.0	2.088310	0.208997	0.524009
0.71	0.4	1.0	2.192459	0.113759	0.530353
0.71	0.7	1.0	2.345613	0.016754	0.539547
0.71	1.0	1.0	2.585153	0.214642	0.552725
0.71	0.5	0.5	2.147838	0.079146	0.522170
0.71	0.5	1.0	2.236659	0.075288	0.533045
0.71	0.5	1.5	2.281870	0.075569	0.538544
0.71	0.5	2.0	2.307403	0.077189	0.541692

Table 3: Numerical values of $f''(0)$, $\theta'(0)$ and $-\varphi'(0)$ for $Gr = Gc = 0.87$, $M = 0.1$, $K = 0.01$, $\alpha = 30^0$, $Pr = 0.71$, $Q = 0.5$, $R = 1.0$, $f_w = 0.5$

Kr	*Sc*	τ	$f''(0)$	$-\theta'(0)$	$-\varphi'(0)$
0.01	0.6	0.1	2.236659	0.075288	0.533045
0.1	0.6	0.1	2.221793	0.074524	0.578133
0.3	0.6	0.1	2.193005	0.073073	0.670121
0.5	0.6	0.1	2.168782	0.071884	0.753061
0.1	0.22	0.1	2.391037	0.088190	0.349239
0.1	0.6	0.1	2.221793	0.074524	0.578133
0.1	0.78	0.1	2.179728	0.071962	0.661986
0.1	1.76	0.1	2.056207	0.066037	1.030045
0.1	0.6	0.1	2.236659	0.075288	0.533045
0.1	0.6	2.0	2.208092	0.073471	0.572966
0.1	0.6	4.0	2.180499	0.071851	0.618500
0.1	0.6	5.0	2.167510	0.071144	0.642471

REFERENCE

[1] Sengupta, T. K., Unnikrishnan, S., Bhaumik, S., Singh, P. and Usman, S., (2011), "Linear spatial stability analysis of mixed convection boundary layer over a heated plate," Progress in Applied Mathematics, vol. 1, pp.71–89. View at Google Scholar

[2] Ali, F. M., Nazar, R., Arifin, N. M. and Pop, I., (2011), "MHD mixed convection boundary layer flow toward a stagnation point on a vertical surface with induced magnetic field," Journal of Heat Transfer, vol.133, no.2, Article ID 022502, pp.1–6. View at Publisher. View at Google Scholar. View at Scopus.

[3] Subhashini, S. V., Samuel, N. and Pop, I., (2011), "Effects of buoyancy assisting and opposing flows on mixed convection boundary layer flow over a permeable vertical surface," International Communications in Heat and Mass Transfer, vol.38, no.4, pp.499–503. View at Publisher · View at Google Scholar · View at Scopus

[4] Lloyd, J. R. and Sparrow, E. M., (1970), "Combined forced and free convection flow on vertical surfaces," International Journal of Heat and Mass Transfer, vol.13, no.2, pp.434–438. View at Publisher · View at Google Scholar · View at Scopus

[5] Schneider, W., (1979), A similarity solution for combined forced and free convection flow over a horizontal plate," International Journal of Heat and Mass Transfer, vol.22, no.10, pp.1401–1406. View at Publisher · View at Google Scholar · View at Zentralblatt MATH · View at Scopus

[6] Wilks, G., (1973), Combined forced and free convection flow on vertical surfaces, International Journal of Heat and Mass Transfer, vol.16, no.10, pp.1958–1964. View at Publisher · View at Google Scholar · View at Zentralblatt MATH · View at Scopus

[7] Yao, L. S., (1987), Two-dimensional mixed convection along a flat plate, Journal of Heat Transfer, vol.109, no.2, pp.440–445. View at Publisher · View at Google Scholar · View at Scopus

[8] Ramachandran, N., Chen, T. S. and Armaly, B. F., (1988), Mixed convection in stagnation flows adjacent to vertical surfaces, Journal of Heat Transfer, vol.110, no.2, pp.373–377. View at Publisher · View at Google Scholar · View at Scopus

[9] Laaroussi, N., Lauriat G. and Desrayaud, G., (2009), Effects of variable density for film evaporation on laminar mixed convection in a vertical channel. International Journal of Heat Mass Transfer, Vol.52, no.1-2, pp.151-164.

[10] Ait Hammou, Z., Benhamou, B., Galanis N. and Orfi, J., (2004), Laminar Mixed Convection of humid Air in a vertical channel with evaporation or

condensation at the wall. International Journal of Thermal Sciences, Vol.43, no.6, pp.531-539.

[11] Said, S. A. M., Habib, M. A., Badr H. M. and Anwar, S., (2005), Turbulent natural convection between inclined isothermal plates. Computers and Fluids, Vol.34, no.9, pp.1025-1039.

[12] Sri Hari Babu, V. and Ramana Reddy, G. V., (2011), mass transfer effects on MHD mixed convective flow from a vertical surface with Ohmic heating and viscous dissipation , Adv. Appl. Sci. Res., Vol.2, no.4, pp.138.

[13] Chen, C.–H., Yunlin, Taiwan, (2004), Heat and mass transfer in MHD flow by natural convection from a permeable, inclined surface with variable wall temperature and concentration, Acta Mechanica, Vol.172, pp.219-235.

[14] Lai, F. C. and Kulacki, F. A., (1991), Non-Darcy Mixed Convection along a Vertical Wall in a Saturated Porous Medium, ASME Journal of Heat Transfer, Vol.113, pp.252-255. http://dx.doi.org/10.1115/1.2910537

[15] Nasir Uddin, Md., Alim M. A. and Chowdhury, M. M. K., (2014), "Effect of Conjugate Heat and Mass Transfer on MHD Mixed Convective Flow past Inclined Porous Plate in Porous Medium", International Journal of Mechanical, Industrial Science and Engineering, vol.08, no.03, pp.1870-1875.

[16] Sattar and Hossain, M., (1992), Unsteady Hydromagnetic Free Convection Flow with Hall Current and Mass transfer along an Accelerated Porous Plate with Time Dependent Temperature and Concentration, Canadian Journal of Physics, Vol.70, No.5, pp.369-375. doi:10.1139/p92-061

[17] Vajravelu, K., (1994), Flow and Heat transfer in a saturated porous medium over a stretching surface, ZAMM, Vol.75, pp.605-614.

[18] Hong, J. T., Tien, C. L. and Kaviany, M., (1985), Non-Darcian effects on vertical-plate natural convection in porous media with high porosities, int.J.Heat Mass Transfer, Vol.28, pp.2149-2175.

[19] Chen, C. K. and Lin, C. R., (1995), Natural convection from an isothermal vertical surface embedded in a thermally stratified high-porosity medium, Int.J.Engg.Sci. Vol.33, pp.131-138.

[20] Jaiswal, B. S. and Soundalgekar, V. M., (2001), Oscillating plate temperature effects on a flow past an infinite vertical porous plate with constant suction and embedded in a porous medium, Heat Mass Transfer, Vol.37, pp.125-131.

[21] Sparrow, E. M. and Cess, R. D., (1955), Hemisphere Publ. Stuart. J. T., Proc. Soc. London, Vol.231, pp.116-121.

[22] Pop, I. and Soundalgekar, V. M., (1962), I.J. Heat Mass transfer, Vol.17, pp.85-92.

[23] Reddy, M. G., Reddy, N. B., (2011), Mass transfer and Heat Generation Effects on MHD Free Convection Flow past an Inclined Vertical Surface in a Porous Medium, J. of Applied Fluid Mechanics, Vol.4, No.3, Issue 1, pp.7-11.

[24] Ramachandra Prasad, V. and Bhaskar Reddy, N., (2008), Radiation effects on an unsteady MHD convective heat and mass transfer flow past a semi – infinite vertical permeable moving plate embedded in a porous medium, Journals of Energy Heat and mass transfer, Vol.30, pp.57-68.

[25] Ramana Reddy, G. V., Ramana Murthy, Ch. V. and Bhaskar Reddy, N., (2010), Mass transfer and radiation effects of unsteady MHD free convective fluid flow embedded in porous medium with heat generation/absorption, Journal of Applied Mathematics and Fluid Mechanics, Vol.2, No.1, pp. 85–98.

[26] Aydin, O. and Kaya, A., (2009), MHD mixed convective heat transfer flow about an inclined plate, Heat Mass Transfer, Vol.46, pp.129-136.

[27] Samad, M. A. and Rahman, M. M., (2006), Thermal Radiation Interaction with Unsteady MHD Flow past a Vertical Porous Plate Immersed in a Porous Medium, J.Nav.Arc.Mar.Eng., Vol.3, pp.7-14.

[28] Uddin, Z., and Kumar, M., (2011), MHD heat and mass transfer free convection flow near the lower stagnation point of an isothermal cylinder imbedded in porous domain with the presence of radiation, Jordan J Mechanical and Industrial Engineering, Vol.5, no.2, pp.133-138.

[29] Singh, H., Ram, P., and Kumar, A., (2011), A study of the effect of chemical reaction and radiation absorption on MHD convective heat and mass transfer flow past a semi-infinite vertical moving plate with time dependent suction, International journal of Applied Mathematical and Mechanics, Vol.7, no.20, pp.38-58.

[30] Ibrahim, F. S., Elaiw, A. M. and Bakr, A. A., (2008), Effect of chemical reaction and radiation absorption on unsteady MHD free convection

flow past a semi-infinite vertical permeable moving plate with heat source/suction, Communication in Non-Linear Science and Numerical Simulation, Vol.13, pp.1056-1066.

[31] Rajeswari, R., Jothiram, B. and Nelson, V. K. (2009), Chemical reaction, heat and mass transfer on linear MHD boundary layer flow through a vertical porous surface in the presence of suction, Applied Mathematical Sciences, Vol.3, pp.2469-80.

[32] Kandasamy, R., Periasamy, K. and Sivagnana Prabhu, K. K., (2005), Chemical Reaction, Heat and Mass Transfer on MHD Flow over a Vertical Stretching Surface with Heat Source and Thermal Stratification Effects, International Journal of Heat and Mass Transfer, Vol.8, no.21-22, pp.4557-4561.

[33] Kandasamy, R., Periasamy, K. and Prabhu, K. K. S., (2005), Effect of Chemical Reaction, Heat and Mass Transfer along a Wedge with Heat Source and Concentration in the Presence of Suction or Injection, International Journal of Heat and Mass Transfer, Vol.48, pp.1388-1394.

[34] Gangadhar, K. and Baskar Reddy, N., (2013), Chemically Reacting MHD Boundary Layer Flow of Heat and Mass Transfer over a Moving Vertical Plate in a Porous Medium with Suction, Journal of Applied Fluid Mechanics, Vol.6, No.1, pp.107-114.

[35] Patil, P. M. and Kulkarni, P. S., (2008), Effects of chemical reaction on free convective flow of a polar fluid through a porous medium in the presence of internal heat generation, Int. J. Therm. Sci.,Vol. 4, pp.1043-1054.

[36] Chamkha, A. J., Pop, I., (2004), Effect of Thermophoresis Particle Deposition in Free Convection Boundary Layer from a Vertical Flat Plate Embedded in a Porous Medium, *Inter. Comm.Heat Mass Transfer*, Vol.31, no.3, pp. 421-430

[37] Bakier, A. J., Mansour, M. A., (2007), Combined of Magnetic Field and Thermophoresis Particle Deposition in Free Convection Boundary Layer from a Vertical Flat Plate Embedded in a Porous Medium, *Thermal Science*, Vol.11, no.1, pp.65-74.

[38] Lin, J. -S., Tsai C. -J. and Chang, C.-P., (2004), Suppression of Particle Deposition in Tube Flow by Thermophoresis *Journal of Aerosol Science*, Vol. 35, No. 2004, pp. 1235- 1250. doi:10.1016/j.jaerosci.2004.05.007

[39] Seddek, M. A., (2005), Finite-Element Method for the Effects of Chemical Reaction, Variable Viscosity, Thermophoresis and Heat Generation/Absorption on a Boundary-Layer Hydromagnetic Flow with Heat and Mass Transfer over a Heat Surface, *Journal of Acta Machanica*, Vol.177, pp.1-18.

[40] Alam, M. S., Rahman, M. M., and Sattar, M. A., (2008), Effects of chemical reactions and thermophoresis on magneto hydrodynamics mixed convective heat and mass transfer flow along an inclined plate in the presence of heat generation and (or) absorption with viscous dissipation and joule heating, Can. J.Phys., Vol.86, pp.1057-1066.

[41] Loganathan, P. and Arasu, P. P., (2010), Thermophoresis Effects on Non-Darcy MHD Mixed Convective Heat and Mass Transfer past a Porous Wedge in The Presence of Suction/Injection, Theoretic Applied Mechanics, Vol. 37, no.3, pp.203-227. doi:10.2298/TAM1003203L.

[42] Talbot, L., Cheng, R. K., Schefer R. W. and Willis, D. R., (1979), Thermophoresis of particles in a heated boundary layer, J. of fluid Mechanics, Vol.101, part.4, pp.737-758.

[43] Brewster, M. Q., (1992), Thermal radiative transfer and properties, John Wiley & Sons, NewYork.